RADIATION DOSE DELIVERED BY ^{125}I, ^{103}PD AND ^{131}CS AND DOSE ENHANCEMENT BY GOLD NANOPARTICLE (GNP) SOLUTION IN PROSTATE BRACHYTHERAPY: A COMPARATIVE ANALYSIS BY MONTE CARLO SIMULATION

HAMDA KHAN[1], UMAIR AZIZ[2*], ZAFAR ULLAH KORESHI[2]

*[1]Department. of Mathematics,
National University of Computer and Emerging Sciences, Islamabad, Pakistan.
[2]Department of Mechatronics Engineering, Air University, Islamabad, Pakistan.*

[*]Corresponding author: umair.aziz@mail.au.edu.pk

ABSTRACT: The energy deposition and radiation dose from commonly used radioisotopes, ^{125}I,^{103}Pd, and ^{131}Cs, used for brachytherapy of cancers is estimated using Monte Carlo (MC) simulations. To enhance the dose, gold nanoparticle (GNP) solutions are injected into the tumor; this results in more effective and shorter therapy duration. It is thus important to estimate the dose enhancement factor (DEF) achievable by a radioisotope. The research presented in this paper thus focuses on a comparative analysis of radioisotopes. To estimate the radiation dose, the Monte Carlo N-particle code MCNP5 was used for a coupled photon-electron simulation of radiation transport from radiation emanating from seeds of radioisotopes implanted in the prostate at positions prescribed to deliver effective doses to the tumor while protecting neighbouring vital organs such as the rectum and urethra. The quantities tallied were the energy deposition (F6 tally) and the pulse heights (*F8 tally) in specified energy bins. The energy deposited in the tumor was used to estimate the absorbed dose to the prostate incorporating the transformations of the radioisotopes during decay. The absorbed dose was subsequently estimated for a GNP-tissue solution with a concentration of 25 mg Au/g of prostate tissue, modelled as a homogenous mixture. From the simulations, it was found that the lifetime absorbed dose is ~96 Gy from 98 seeds, each of 0.31 mCi, of 125I; ~102 Gy, from 115 seeds, each of 1.4 mCi, of 103Pd, and ~90 Gy from ^{131}Cs seeds replacing 103Pd seeds of the same initial activity. The main advantage of ^{131}Cs, over ^{125}I and ^{103}Pd, is observed in the larger dose rate (~26 cGy/hr) delivered initially i.e. in the first few days which is 1.5 and 5.7 times higher than that for ^{103Pd} and ^{125I}. The absorbed dose for 125I, 103Pd and 131Cs increases to ~245, ~130, ~187 Gy respectively with GNP-tissue solution of 25 mg Au/g tissue. From the analysis, it is found that while the lifetime absorbed dose of all three radioisotopes is of the same order, there are advantages in using ^{131}Cs; these advantages are further quantified.

ABSTRAK: Pemendapan tenaga dan dos sinaran radiasi daripada radioisotop yang biasa digunakan, ^{125}I,^{103}Pd, dan ^{131}Cs, digunakan bagi terapibraki kanser dianggar menggunakan simulasi Monte Carlo (MC). Bagi meningkatkan dos, larutan partikel nano emas (GNP) telah disuntik ke dalam tumor; ini lebih memberi kesan dan mengurangkan masa terapi. Oleh itu, adalah penting menganggar faktor dos penggalak (DEF) dapat dicapai dengan radioisotop. Kajian ini mengfokuskan pada analisis perbandingan radioisotop. Bagi menganggarkan dos radiasi, kod Monte Carlo N-partikel MCNP5 telah digunakan pada simulasi pasangan foton-elektron pengangkutan radiasi daripada

pancaran radioaktif benih radioisotop yang ditanam dalam prostat pada posisi yang disebut bagi mencetuskan dos penghantaran yang berkesan pada sel tumor. Dalam masa sama melindungi organ penting seperti rektum dan uretra. Kuantiti diselaras dengan pemendapan tenaga (selaras F6) dan ketinggian denyut (selaras *F8) dalam aras tenaga sebenar. Tenaga yang dienap dalam sel tumor ini telah digunakan bagi menganggarkan dos serapan pada prostat dengan menggabungkan transformasi radioisotop ketika susutan. Dos yang diserap telah kemudiannya dianggarkan bagi larutan tisu-GNP dengan ketumpatan 25 mg Au/g tisu prostat, dimodelkan sebagai campuran homogen. Daripada simulasi, dapatan kajian menunjukkan dos diserap sebanyak ~96 Gy daripada 98 benih, setiap satu daripada 0.31 mCi, 125I; ~102 Gy, dari 115 benih, setiap 1.4 mCi, dari 103Pd, dan ~90 Gy daripada benih ^{131}Cs menggantikan benih 103Pd pada pemulaan aktiviti yang sama. Keistimewaan utama adalah ^{131}Cs, ke atas ^{125}I dan ^{103}Pd, telah dilihat dalam kadar dos lebih besar (~26 cGy/hr) dikeluarkan pada pemulaannya iaitu dalam beberapa hari pertama iaitu 1.5 dan 5.7 kali lebih tinggi daripada ^{103Pd} dan ^{125I}. Dos yang diserap pada 125I, 103Pd dan 131Cs bertambah kepada ~245, ~130, ~187 Gy masing-masing dengan larutan tisu-GNP sebanyak 25 mg Au/g tisu. Hasil analisis menunjukkan penyerapan seumur hidup dos diserap pada ketiga-tiga radioisotop dalam aturan yang sama, ini adalah keistimewaan menggunakan ^{131}Cs; keistimewaan ini akan terus diuji pada masa depan dan diukur kuantitinya.

1. INTRODUCTION

Cancer cases globally are expected to grow from 14.1 million in 2012 to 24 million by 2035 [1, 2] with the top three: lung [3], prostate [4-6], and colorectal cases accounting for over 47% of all cancers in men. The treatments for cancer, in order of general preference, are chemotherapy, surgery, and radiation therapy. In the case of recurrent cancers however, brachytherapy is the preferred treatment due to its localized and non-invasive effects.

For brachytherapy, radioisotopes with energy <50 keV, such as ^{125}I and ^{103}Pd sources [7-9] with typical implants of 50-80 metallic seeds encasing isotopes, are used as low dose rate (LDR) [10] therapies for the treatment of prostate cancer, uveal melanomas and brain tumours. The dose is estimated by a number of computer codes such as EGSnrc, GEANT[11], PENELOPE [12] and MCNP [13] based on Monte Carlo (MC) methods [14].

Further improvements in the effectiveness of brachytherapy are being considered by the injection of gold nanoparticles through fenestrations of cancer cells. The particle size requirements are in the nanoscale range (~10^{-9} m) which is comparable with the diameter of an atom (~10^{-10} m) [15, 16].

For MC simulations in brachytherapy, it has been demonstrated that DEF is a function of the source energy and concentration of GNP solution [17-20], while the size of GNPs is not so important (above the K-edge energy). Thus, in this work, a homogenous model with considerable savings on the computational effort, required for a full heterogeneous model, is used to extract crucial information on the DEF resulting from the presence of gold in small concentration while MCNP has the capability of modelling very detailed heterogeneous configurations. This paper considers a homogenous model solely for the purpose of carrying out a comparative study for the dose delivered to a prostate tumour by ^{125}I, ^{103}Pd and ^{131}Cs and particularly the enhancement of radiation dose due to the presence of gold.

The ultimate goal of brachytherapy is to deliver maximum dose to the tumour while minimizing collateral damage to the normal tissue and for maximizing the DEF, there is still no consensus on the optimal size, shape and distribution of GNPs. However, experimental and pre-clinical evidence for mouse tumours, showing a 1-year survival rate of 86% following a dose of 26 Gy with 1.9 nm intravenously administered GNPs *vs* 20% for tumours not laden with GNPs [15], indicate that nanotechnology offers promising improvements in brachytherapy.

The radioisotope cesium-131 (^{131}Cs), was introduced to brachytherapy in 2004 [21] and in the first five years it was used in about 3000 prostate implants yielding the required dose in less time compared with ^{125}I and ^{103}Pd due to its shorter half-life and high energy, as shown in Table 1.

Table 1: Energy and half-life of ^{125}I, ^{103}Pd and ^{131}Cs

Radionuclide	E (keV)	T$_{1/2}$ (days)
^{103}Pd	20.8	17
^{125}I	35.49	59.4
^{131}Cs	29-30.4	9.7

Typically, ^{125}I is used with a radiation dose of 145 Gy or more conforming to the prescribed dose of 145 Gy suggested by the American Association of Physicists in Medicine Task Group 64 [22].

While all three are low-energy sources, so that their dose would not extend to normal tissue in nearby organs [23], one of the main advantages of ^{131}Cs is that it offers an initial dose rate of ~32 cGy/h at the periphery [24] which is 1.5 and 4 times higher than that from ^{103}Pd and ^{125}I respectively. This initial dose rate advantage is a vital radiobiological parameter for rapidly growing tumours [25] as well as for slow-growing tumours such as prostate adenocarcinomas. A set of clinical recommendations for prescribed doses, on the basis of 1200 prostate implants [26] indicated that the high initial dose rate of ^{131}Cs caused more intense urinary and rectal complication but they also resolved more quickly than that for ^{125}I and ^{103}Pd. That study also found that the drop in prostate-specific antigen levels from ^{131}Cs, with a maximum follow-up of just over three years and median follow-up of 23 months, were equivalent to that from other isotopes. Such promising results from ^{131}Cs extended its use to gynecological malignancies [27] and to brain radiotherapy [28] from which it was demonstrated that this treatment was well-tolerated and safe for patients.

2. MATERIALS AND METHODS

2.1 Monte Carlo Simulation

The Monte Carlo code MCNP5 is used to carry out a coupled photon-electron simulation of radiation transport in the range 1 keV-100 MeV to estimate the radiation dose distribution for prostate tumor brachytherapy. The radioisotope sources considered are ^{125}I, ^{103}Pd and ^{131}Cs in the form of 'seeds' modelled as point sources. For ^{125}I, 98 seeds each of 0.31 mCi and for ^{103}Pd 115 seeds each of 1.4 mCi were spatially distributed in the tumour tissue, as shown in Fig. 1 [29] for data given for two patients with different size prostates. The placement of needles takes into account a number of factors including the location of vital organs surrounding the prostate, such as the bladder, urethra, and rectum.

For simulating the effect of ^{131}Cs, the ^{103}Pd seeds were replaced by ^{131}Cs seeds of the same initial activity and spatial distribution. The energy deposition track length estimation tally F6 and the pulse height tally *F8 are both used for estimating energy deposition to get reliable estimates in case of a few interactions in a region of interest. The simulation is repeated with gold-tissue solution; material compositions for both simulations are listed in Table 1. The photon and electron data for both tissue and gold are based on ENDF/B-VI (Release 8).

In MCNP the "detailed physics" simulation incorporates coherent (Thomson) scattering and fluorescent photons produced from photoelectric absorption. Electrons produced from photon collisions are transported in a "condensed history" method that accumulates the effects of many individual collisions into single steps sampled probabilistically. The effects of such artefacts for electron transport have been investigated [30-32] with EGSnrc, GEANT and PENELOPE codes and in some cases "large discrepancies" (>3%) have been found between MCNP5 dose distributions and the 'reference codes' concluding that MCNP5 electron transport calculations are not accurate at all energies and in every medium by general clinical standards. It can thus be anticipated that MCNP5 may differ due to its inadequate low-energy treatment of electron transport. Authors of [33] have carried out electron transport comparisons of MCNPX, Penelope and EGSnrc, for electrons of 20-450 keV in water, lead, and tungsten. These comparisons were focused on bremsstrahlung, energy deposition in matter, electron ranges and production of secondary electrons by gamma radiation.
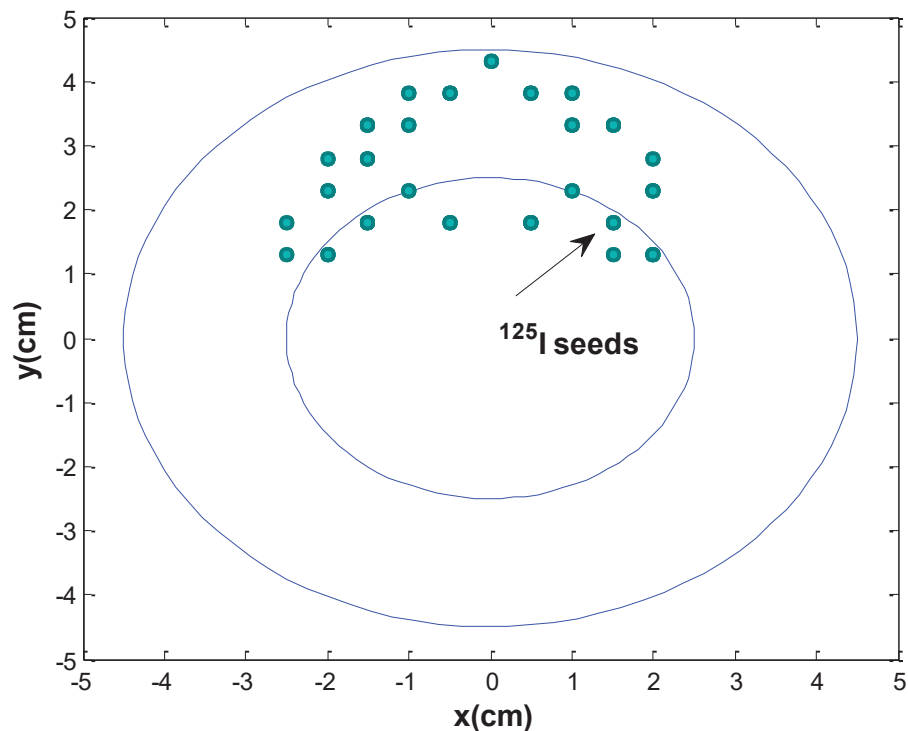

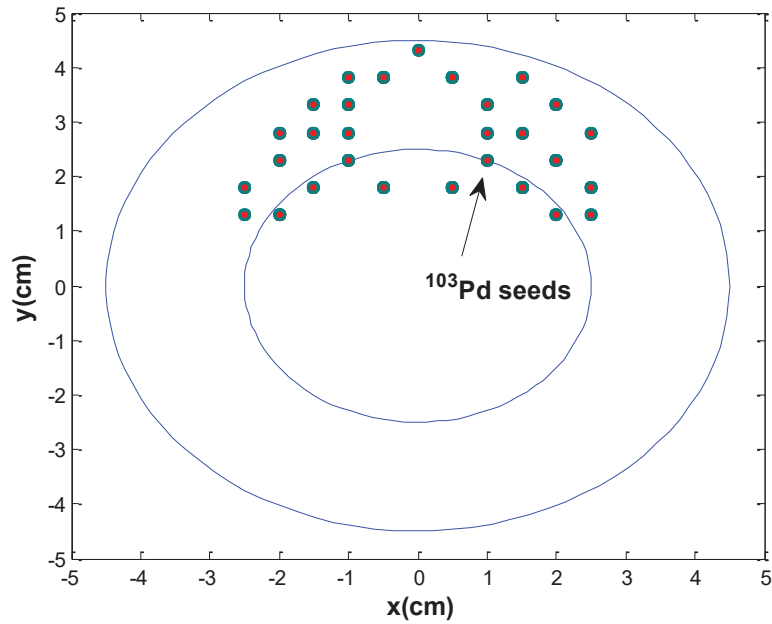Fig. 1: Placement of 25 needles with 98 seeds of ^{125}I in the x-y plane.

Fig. 2: Placement of 29 needles of 115 seeds of ^{103}Pd/^{131}Cs in the x-y plane.

The F6 tally for dose

$$D = \frac{\rho}{m} \int dE \int dt \int dV \int d\Omega \; \sigma_t(E)H(E)\phi(\bar{r},\widehat{\Omega},E,t) \, \text{MeV g}^{-1}$$

from MCNP is converted from MeV/g to yield the dose rate in Gy/hr by using the activity as shown below.

2.2 Activity and Transformations

The activity of a radioisotope is $A(t) = A_o e^{-\lambda t}$ and the number of transformations in an interval $\tau = t_2 - t_1$ is thus

$$\text{Tr}(t_1, t_2) = \frac{A(t_1)}{\lambda}\left(1 - e^{-\lambda \tau}\right) \tag{1}$$

Thus the 'infinite-time' transformations i.e. the number of disintegrations integrated over the time interval $(0, \infty)$ is A_o/λ.

The absorbed dose is computed as follows:

$$\text{Abs Dose} = 1.6 \; X \; 10^{-10} \frac{A_o}{\lambda} \frac{NE}{m} \; \text{Gy} \tag{2}$$

where A_o is the initial activity, N is the number of radioisotope seeds, and E is the energy pulse height (*E8) tally (MeV) and m is the mass of the tumor (g).

Thus, the absorbed dose varies directly with the energy deposition and source, which in turn depends on the number of transformations i.e. the product of initial activity and half-life.

3.   RESULTS

MCNP simulations were carried out on an Intel(R) Core (TM) i7-2620M CPU @ 2.70GHz with an installed memory of 8.00 GB (3.24 GB usable) and 32-bit Operating system with Windows 7 Professional. The runtime for each simulation of 10^7 source particles was 35.60, 51.1 and 41 minutes for ^{125}I, ^{103}Pd and ^{131}Cs, respectively

The time-dependent transformations and activities of ^{125}I, ^{103}Pd and ^{131}Cs, for an initial activity of 1 mCi each, are shown in Fig. 3. The basic hypothesis for effectiveness of each isotope arises from its half-life. This factor results in a longer decay time for ^{125}I while faster decay rates of ^{103}Pd and ^{131}Cs translate into lifetime transformations of 2.74×10^{14}, 7.84×10^{13} and 4.47×10^{13} for ^{125}I, ^{103}Pd and ^{131}Cs respectively which clearly illustrate the slow build-up, but higher dose from ^{125}I after ~ six months compared with the much faster effects of ^{103}Pd and ^{131}Cs. There is hence a saturation in activities for ^{103}Pd and ^{131}Cs with the implications that the effect of these two isotopes is seen much faster than that for ^{125}I.

Figure 4 shows the absorbed dose for ^{125}I (initial activity 0.31 mCi, 98 seeds distributed as illustrated in Fig. 1), ^{103}Pd and ^{131}Cs (both of initial activity 1.4 mCi 115 seeds distributed as illustrated in Fig. 2) which indicates that ^{131}Cs is clearly the best in terms of delivering the highest and fastest dose to the tumour, reaching 50 Gy in the first 10 days and 100 Gy when GNPs in a solution of 25 mg/g tissue are injected in the tumour. The absorbed dose on a longer timescale, however, is highest for ^{125}I with GNP solution but exceeds that from ^{131}Cs after about three months. For the sake of comparison, when all seeds are of equal initial activity (1.4 mCi) and placed in the configuration of Fig. 2, it is seen in Fig. 5 that the highest absorbed dose for both cases, with and without GNP-solution, is the highest at 117 Gy and ~283 Gy respectively but after ~250 days). Thus for a given requirement, ^{125}I exceeds the ^{103}Pd dose in about 200 days; higher doses for stronger tumours can thus not be treated by ^{131}Cs and ^{103}Pd unless they are used in conjunction with gold solutions.
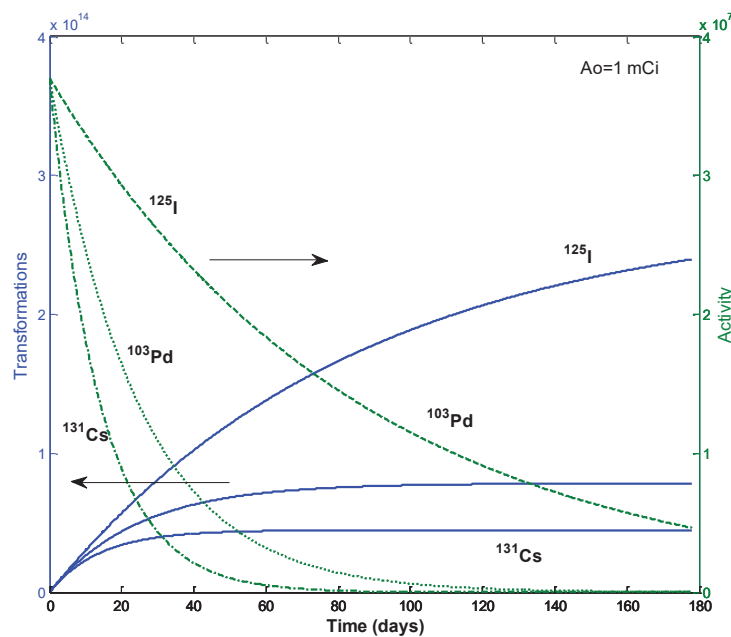

Fig. 3: Transformations and activity of ^{125}I, ^{103}Pd and ^{131}Cs each of
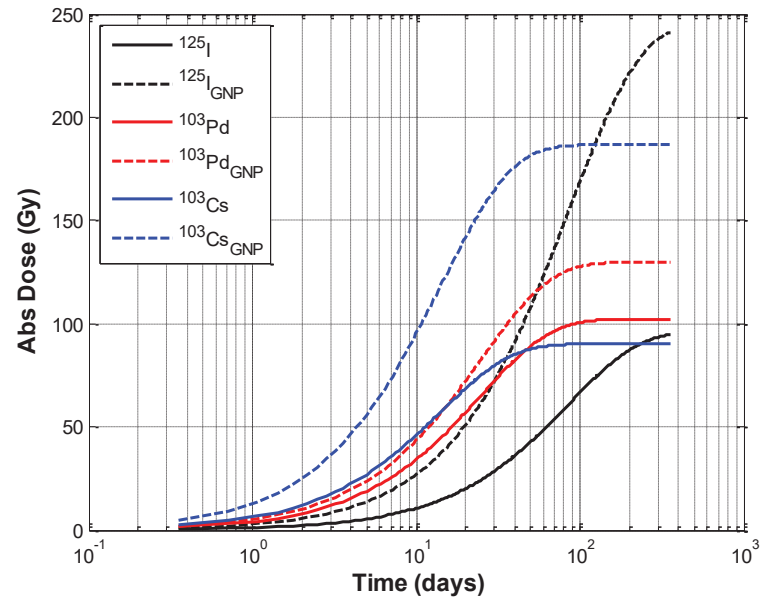initial activity 1 mCi.

Fig. 4: Absorbed dose (Gy) as a function of time (days) in prostate tissue from 98 seeds each of 0.31 mCi of ^{125}I, 115 seeds each of 1.4 mCi of ^{103}Pd and 115 seeds each of 1.4 mCi ^{131}Cs (replacing ^{103}Pd seeds).
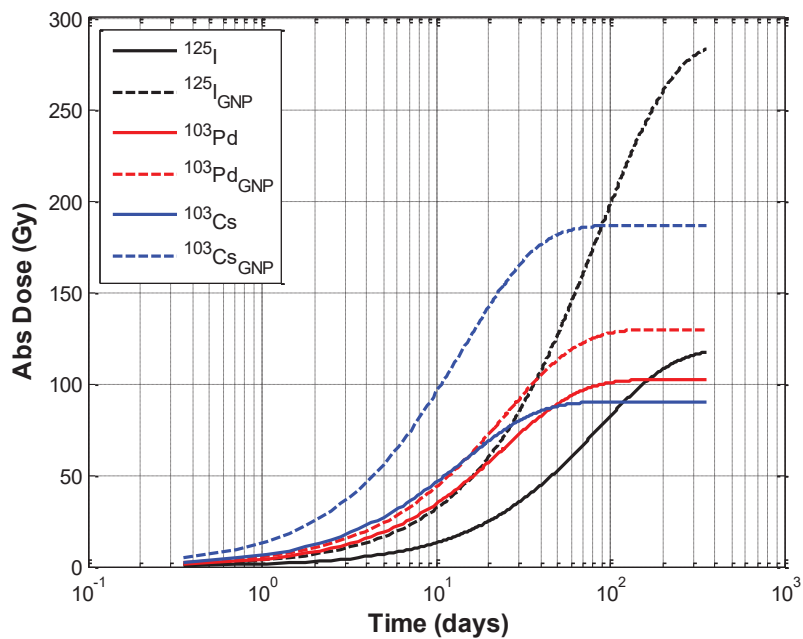

Fig. 5: Absorbed dose (Gy) as a function of time (days) in prostate tissue from ^{125}I, ^{103}Pd and ^{131}Cs (115 seeds each of 1.4 mCi distributed as in Fig. 2)

On a shorter time scale, the differences between all three isotopes is seen from the absorbed dose rates shown in Fig. 6 showing a clear advantage of ^{131}Cs over the first ~300 hours exceeding 5.7 times and 1.5 times that of ^{125}I and ^{103}Pd respectively in the initial period and falling gradually, as shown in Fig. 7. Levelling off is found to be ~300 and ~400 hours respectively for ^{103}Pd and ^{125}I.
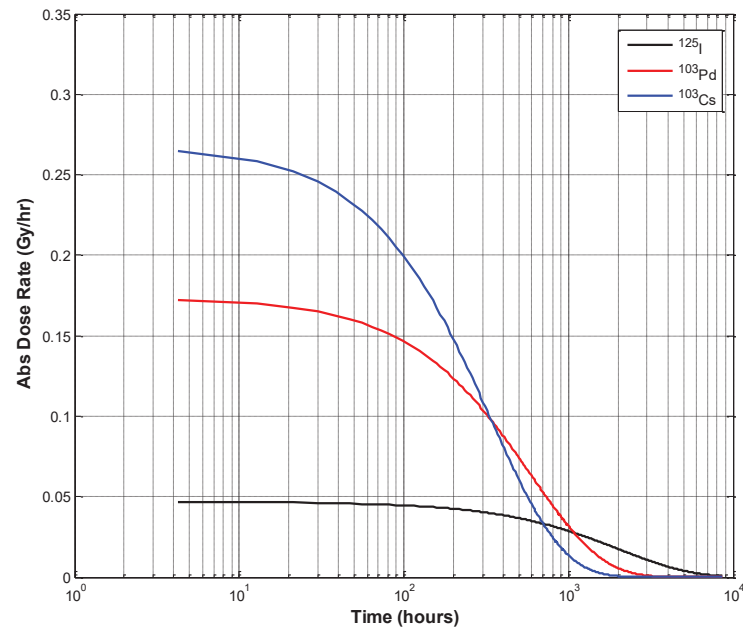
Fig. 6: Absorbed dose rate (Gy/hr) as a function of time (hours) in prostate tissue from 98 seeds each of 0.31 mCi of ^{125}I, 115 seeds each of 1.4 mCi of ^{103}Pd and 115 seeds each of 1.4 mCi ^{131}Cs (replacing ^{103}Pd seeds).

Fig. 7: Relative absorbed dose rate (Gy/hr) of ^{131}Cs (relative to ^{125}I and ^{103}Pd) as a function of time (hours) in prostate tissue from 98 seeds each of 0.31 mCi of ^{125}I, 115 seeds each of 1.4 mCi of ^{103}Pd and 115 seeds each of 1.4 mCi ^{131}Cs (replacing 103Pd seeds).

The lifetime dose delivered by the three sources considered is shown in Table 2. The absorbed dose for ^{125}I, ^{103}Pd and ^{131}Cs increases from 96.30, 102.21 and 90 Gy to ~245, ~130, ~187 Gy with GNP-tissue solution of 25 mg Au/g tissue. These results are in line

with the decay rates of the three isotopes which favour ^{125}I in terms of energy but result in a slow dose delivery.

The dose enhancement with gold GNP-tissue found in these simulations is the effect of both source energy of each radioisotope and the solution concentration. The important photon interaction for high-Z materials such as gold is the photoelectric effect for which the cross-section varies as $\mu_{PE} \sim \frac{\rho Z^3}{E^3}$ so that low energy and high-Z are desirable for dose enhancement which is localized to the tumor due to the short range of photoelectrons and Auger electrons in the surrounding medium which for electrons of energy 0.1 MeV is ~100 microns in water and ~15 microns in gold so that the effect of gold will require thin layers (of the order of $\ll$ 100 nm) to utilize the energy of photoelectrons in water. At this energy, the photoabsorptions were estimated to be ~13.5% of all interactions. Thus, the increases found in this work are a measure of the photon interaction in each radioisotope. As shown in Table 2, the highest dose achievable is ~245 Gy by ^{125}I, and lesser doses by ^{103}Pd and ^{131}Cs for 25 mg Au/g tissue.

When the configuration of Fig. 2 is used for all three sources of 1.4 mCi each, the F6 and F8 tallies for ^{125}I increase to 1.82733×10^{-5} (0.0011) MeV/g and 1.24662×10^{-3} (0.0016) MeV respectively, as depicted in Fig. 5.

Table 2: Lifetime absorbed dose (Gy) to prostate tumour due to ^{125}I, ^{103}Pd and ^{131}Cs. The second result in F6, F8 and Abs. Dose columns refer to Tissue with 25 mg Au/g tissue homogenous mixture

Source	$T_{1/2}$ (d)	A_0 (mCi)	E(kev) N_{seeds}	Tr=A_0/λ (s^{-1})	F6 (rel. err.) (MeV/g)	F8 (rel. err.) (MeV)	Abs. Dose* (Gy)
^{125}I	59.4	0.31	35.49	8.5×10^{13}	1.73548×10^{-5} (0.0011)	1.183×10^{-3} (0.0016)	96.30
			98		4.30593×10^{-5} 0.0012	3.0087×10^{-3} 0.0010	244.91
^{103}Pd	17	1.4	20.8	1.1×10^{14}	1.21460×10^{-5} (0.0018)	8.2786×10^{-4} (0.0015)	102.21
			115		1.50096×10^{-5} 0.0019	1.0511×10^{-3} 0.0014	129.77
^{131}Cs	9.7	1.4	30.4	6.3×10^{13}	1.88145×10^{-5} (0.0012)	1.2803×10^{-3} (0.0015)	90.17
			115		3.79186×10^{-5} (0.0013)	2.64847×10^{-3} 0.0010	186.57

*for an organ mass 16.3634 g

4. CONCLUSIONS

From the simulations, it was concluded that:

- lifetime absorbed dose is ~96 Gy from 98 seeds, each of 0.31 mCi, of ^{125}I, ~102 Gy, from 115 seeds, each of 1.4 mCi, of ^{103}Pd, and ~90 Gy from ^{131}Cs seeds replacing ^{103}Pd seeds of the same initial activity,

- there is a saturation in the activities of ^{103}Pd and ^{131}Cs with the implications that the effect of these two isotopes is much faster than that of ^{125}I,

- the main advantage of ^{131}Cs, is the larger initial dose rate (~26 cGy/hr) for the first few days, which is 1.5 and 5.7 times higher than that for ^{103}Pd and ^{125}I,

- with a GNP-tissue mixture, the dose enhancement factors in ^{125}I, ^{103}Pd and ^{131}Cs are 2.5, 1.26 and 2.1 respectively which give another edge to ^{131}Cs,

- for a specified dose, ^{125}I exceeds ^{103}Pd by about 200 days; higher doses for stronger tumours can thus not be treated by ^{131}Cs and ^{103}Pd unless they are used in conjunction with gold solutions.

This work has shown results for three candidate radioisotopes in their effectiveness for the treatment of tumours. The basic hypotheses to determine their effectiveness were their radiation energy and half-life. The Monte Carlo simulations carried out in this work have elaborated the effect of radiations from three isotopes and found substantially higher time of treatment, as well as stronger radiation dose with ^{125}I than for ^{103}Pd and ^{131}Cs.

FUNDING

REFERENCES

[1]   Common cancer types, national cancer institute [https://www.cancer.gov/types/common-cancers]

[2]   Worldwide cancer data, world cancer research fund.
      [https://www.wcrf.org/dietandcancer/cancer-trends/worldwide-cancer-data]

[3]   Yu E, Lewis C. (2018) Lung cancer brachytherapy. Current Cancer Therapy Reviews, 14(2): 137-148.   doi: 10.2174/1573394714666180208145420.

[4]   Blanchard P, Pugh TJ, Swanson DA, Mahmood U, Chen HC, Wang X, Graber WJ, Kudchadker RJ, Bruno T, Feeley T, Frank SJ. (2018) Patient-reported health-related quality of life for men treated with low-dose-rate prostate brachytherapy as monotherapy with 125-Iodine, 103-Palladium, or 131-Cesium: Results of a prospective phase ii study. Brachytherapy, 17(2): 265-276.   doi: 10.1016/J.BRACHY.2017.11.007.

[5]   Rice SR, Olexa G, Hussain A, Mannuel H, Naslund MJ, Amin P, Kwok Y. (2019) A phase ii study evaluating bone marrow-sparing, image-guided pelvic intensity-modulated radiotherapy (IMRT) with Cesium-131 brachytherapy boost, adjuvant chemotherapy, and long-term hormonal ablation in patients with high risk, nonmetastatic prostate cancer. American Journal of Clinical Oncology, 42(3): 285-29.   doi: 10.1097/COC.0000000000000520.

[6]   Fahmi MR, Hashikin NA, Yeong CH, Guatelli S, Ng KH, Malaroda A, Rosenfeld AB, Perkins AC. (2019) Evaluation of organ doses following prostate treatment with permanent brachytherapy seeds: A geant4 Monte Carlo simulation study. Journal of Physics: Conference Series, 1248(1): 012049-012049.   doi: 10.1088/1742-6596/1248/1/012049.

[7]   Radioisotopes in medicine, world nuclear association [https://www.world-nuclear.org/information-library/non-power-nuclear-applications/radioisotopes-research/radioisotopes-in-medicine.aspx]

[8]   Park DS. (2012) Current status of brachytherapy for prostate cancer. Korean Journal of Urology, 53(11): 743-749.   doi: 10.4111/kju.2012.53.11.743.

[9]   Lechtman E, Mashouf S, Chattopadhyay N, Keller BM, Lai P, Cai Z, Reilly RM, Pignol JP. (2013) A Monte Carlo-based model of gold nanoparticle radiosensitization accounting for increased radiobiological effectiveness. Physics in Medicine and Biology, 58(10): 3075-3087.   doi: 10.1088/0031-9155/58/10/3075.

[10] Stish BJ, Davis BJ, Mynderse LA, McLaren RH, Deufel CL, Choo R. (2018) Low dose rate prostate brachytherapy. Translational Andrology and Urology, 7(3): 341-356. doi: 10.21037/tau.2017.12.15.

[11] Allison J, Amako K, Apostolakis J, Araujo H, Arce Dubois P, Asai M, Barrand G, Capra R, Chauvie S, Chytracek R, Cirrone GAP, Cooperman G, Cosmo G, Cuttone G, Daquino GG, Donszelmann M, Dressel M, Folger G, Foppiano F, Generowicz J, Grichine V, Guatelli S,

Gumplinger P, Heikkinen A, Hrivnacova I, Howard A, Incerti S, Ivanchenko V, Johnson T, Jones F, Koi T, Kokoulin R, Kossov M, Kurashige H, Lara V, Larsson S, Lei F, Link O, Longo F, Maire M, Mantero A, Mascialino B, McLaren I, Mendez Lorenzo P, Minamimoto K, Murakami K, Nieminen P, Pandola L, Parlati S, Peralta L, Perl J, Pfeiffer A, Pia MG, Ribon A, Rodrigues P, Russo G, Sadilov S, Santin G, Sasaki T, Smith D, Starkov N, Tanaka S, Tcherniaev E, Tome B, Trindade A, Truscott P, Urban L, Verderi M, Walkden A, Wellisch JP, Williams DC, Wright D, Yoshida H. (2006) Geant4 developments and applications. IEEE Transactions on Nuclear Science, 53(1): 270-278. doi: 10.1109/TNS.2006.869826.

[12] Salvat F, José M, Sempau J. (2011) Penelope 2011: a code system for monte carlo simulation of electron and photon transport. Nuclear Energy Agency, doc(2011)5. https://www.oecd-nea.org/science/docs/2011/nsc-doc2011-5.pdf

[13] Briesmeister JF. (2000) Mcnp: a general monte carlo n-particle transport code. version 4c, LA-13709-M. https://permalink.lanl.gov/object/tr?what=info:lanl-repo/lareport/LA-13709-M

[14] Kalos MH, Whitlock PA. (2008) Monte Carlo methods. Wiley-Blackwell, 2008, pp. 203-203.

[15] Jain S, Hirst DG, O'Sullivan JM. (2012) Gold nanoparticles as novel agents for cancer therapy. The British Journal of Radiology, 85(1010): 101-113. doi: 10.1259/bjr/59448833.

[16] Chatterjee DK, Wolfe T, Lee J, Brown AP, Singh PK, Bhattarai SR, Diagaradjane P, Krishnan S. (2013) Convergence of nanotechnology with radiation therapy-insights and implications for clinical translation. Translational Cancer Research, 2(4): 256-268. doi: 10.3978/j.issn.2218-676X.2013.08.10.

[17] Lechtman E, Chattopadhyay N, Cai Z, Mashouf S, Reilly R, Pignol JP. (2011) Implications on clinical scenario of gold nanoparticle radiosensitization in regards to photon energy, nanoparticle size, concentration and location. Physics in Medicine and Biology, 56(15):4631-4647. doi: 10.1088/0031-9155/56/15/001.

[18] Mesbahi A, Jamali F, Garehaghaji N. (2013) Effect of photon beam energy, gold nanoparticle size and concentration on the dose enhancement in radiation therapy," BioImpacts : BI, 3(1): 29-35. doi: 10.5681/bi.2013.002.

[19] Asadi S, Vaez-zadeh M, Masoudi SF, Rahmani F, Knaup C, Meigooni AS. (2015) Gold nanoparticle-based brachytherapy enhancement in choroidal melanoma using a full monte carlo model of the human eye. Journal of Applied Clinical Medical Physics, 16(5): 344-357. doi: 10.1120/jacmp.v16i5.5568.

[20] Banoqitah E, Djouider F. (2016) Dose distribution and dose enhancement by using gadolinium nanoparticles implant in brain tumor in stereotactic brachytherapy. doi: 10.1016/j.radphyschem.2016.06.002.

[21] Kehwar TS. (2009) Use of cesium-131 radioactive seeds in prostate permanent implants. Journal of Medical Physics, 34(4): 191-193. doi: 10.4103/0971-6203.56077.

[22] Yu Y, Anderson LL, Li Z, Mellenberg DE, Nath R, Schell MC, Waterman FM, Wu A, Blasko JC. (1999) Permanent prostate seed implant brachytherapy: Report of the american association of physicists in medicine task group no. 64. Medical Physics, 26(10): 2054-2076. doi: 10.1118/1.598721.

[23] Awan SB, Hussain M, Dini SA, Meigooni AS. (2008) Historical review of interstitial prostate brachytherapy," vol. 5. http://ijrr.com/article-1-345-en.pdf

[24] Yaparpalvi R. *et al.* (2007) Is Cs-131 or I-125 or Pd-103 the "ideal" isotope for prostate boost brachytherapy?– A dosimetric view point. International Journal of Radiation Oncology*Biology*Physics, 69(3): S677-S678. doi: 10.1016/J.IJROBP.2007.07.2038.

[25] Armpilia CI, Dale RG, Coles IP, Jones B, Antipas V. (2003) The determination of radiobiologically optimized half-lives for radionuclides used in permanent brachytherapy implants. International Journal of Radiation Oncology, Biology, Physics, 55(2): 378-385. [Online]. Available: http://www.ncbi.nlm.nih.gov/pubmed/12527051.

[26] Bice WS, Prestidge BR, Kurtzman SM, Beriwal S, Moran BJ, Patel RR, Rivard MJ, Cesium Advisory G. (2008) Recommendations for permanent prostate brachytherapy with 131cs: A

consensus report from the cesium advisory group. Brachytherapy, 7(4): 290-296. doi: 10.1016/j.brachy.2008.05.004.

[27]   Wooten CE, Randall M, Edwards J, Aryal P, Luo W, Feddock J. (2014) Implementation and early clinical results utilizing Cs-131 permanent interstitial implants for gynecologic malignancies. Gynecologic Oncology, 133(2): 268-273.   doi: 10.1016/j.ygyno.2014.02.015.

[28]   Wernicke AG, Smith AW, Taube S, Yondorf MZ, Parashar B, Trichter S, Nedialkova L, Sabbas A, Christos P, Ramakrishna R, Pannullo SC, Stieg PE, Schwartz TH. (2016) Cesium-131 brachytherapy for recurrent brain metastases: Durable salvage treatment for previously irradiated metastatic disease. Journal of Neurosurgery, 126(4): 1212-1219.   doi: 10.3171/2016.3.jns152836.

[29]   Usgaonker SR. (2004) MCNP modeling of prostate brachytherapy and organ dosimetry. [Online]. Available: https://oaktrust.library.tamu.edu/handle/1969.1/305.

[30]   Almansa JF, Guerrero R, Al-Dweri FMO, Anguiano M, Lallena AM. (2006) Dose distribution in water for monoenergetic photon point sources in the energy range of interest in brachytherapy: Monte carlo simulations with penelope and geant4. [Online]. Available: http://fm137.ugr.es/PhotonPointSources/

[31]   Archambault JP, Mainegra-Hing E. (2015) Comparison between egsnrc, geant4, mcnp5 and penelope for mono-energetic electron beams. Physics in Medicine and Biology, 60(13): 4951-4962.   doi: 10.1088/0031-9155/60/13/4951.

[32]   Koivunoro H, Siiskonen T, Kotiluoto P, Auterinen I, Hippeläinen E, Savolainen S. (2012) "Accuracy of the electron transport in MCNP5 and its suitability for ionization chamber response simulations: A comparison with the egsnrc and penelope codes. Medical Physics, 39(3): 1335-1344.   doi: 10.1118/1.3685446.

[33]   Šídlová V, Trojek T. (2010) Testing Monte Carlo computer codes for simulations of electron transport in matter. Applied Radiation and Isotopes, 68(4-5): 961-964. doi: 10.1016/j.apradiso.2009.12.019.